The spin evolution of accreting and radio pulsars in binary systems
Nielsen, A.B.

Citation
Nielsen, A. B. (2018, September 13). *The spin evolution of accreting and radio pulsars in binary systems*. Retrieved from https://hdl.handle.net/1887/65380

Cover Page

Universiteit Leiden

The handle http://hdl.handle.net/1887/65380 holds various files of this Leiden University dissertation.

Author: Nielsen, A.B.
Title: The spin evolution of accreting and radio pulsars in binary systems
Issue Date: 2018-09-13

1

Introduction

Neutron stars were mentioned for the first time by Baade & Zwicky (1934) as the end products of massive stars, after a supernovae explosion. The first pulsar was discovered in 1967, at Cambridge University, by Jocelyn Bell Burnell and Anothony Hewish (Hewish et al. 1968). This was, early on, used as the proof of the existence of neutron stars. The discovery led to the Nobel prize in physics awarded to Anthony Hewish and Martin Ryle in 1974. With the detection of the first pulsar followed multiple new discoveries, e.g. the double pulsar system, B1913+16, discovered by Russel Hulse and Joseph Taylor in 1974 (Hulse & Taylor 1975). This binary pulsar was used as an astrophysical laboratory to demonstrate the existence of gravitational waves. Indeed it could be shown that the orbital period of the binary was decaying, following the prediction of general relativity, due to loss of angular momentum carried away by gravitational waves. Russel Hulse and Joseph Taylor were awarded the Nobel prize in physics in 1993. Since these two ground breaking discoveries the pulsar zoo has been expanded to include accreting systems that show pulsations in X-ray and systems that show pulsations in both γ-rays and optical (Wijnands & van der Klis 1998; Shearer & Golden 2002; Smith et al. 2017). With this thesis I study some of the peculiar and puzzling behaviors we observe in binary systems with a pulsar.

1.1   Formation of neutron stars

Neutron stars are some of the most extreme objects in our Universe and they form through a violent process. Towards the end of the evolution of a high mass star, the star transforms silicon to iron in the core, and when the mass of the iron core exceeds the Chandrasekhar limit of $\lesssim 1.4\,M_\odot$, the core starts to collapse (Heger & Woosley 2003; Rosswog & Brüggen 2011). The initial collapse of the core happens so quickly that the outer layers of the star are not immediately affected. The core rebounds from the collapse and sends out a shock wave through the star. This shock wave is the supernova explosion, that disrupts the star, and it is only at this point that the outer layers of the star are affected (Rosswog & Brüggen 2011). The above is a rough description of a core-collapse supernova explosion. The remnants of these supernova explosions are either neutron stars or black holes. For the purpose of this thesis I will focus on neutron star remnants only.

Neutron stars formed in core-collapse supernova are thought to have a high initial spin, close to the break-up spin limit (Heger & Woosley 2003; Heger et al. 2004). Unevolved massive stars rotate fast, at around $200\,\mathrm{km\,s^{-1}}$ (Heger et al. 2004). The contraction of the core, leading up to the supernova explosion, leads to faster rotation, but other processes play a role in the rotation of the core, such as e.g. viscosity and the magnetic field, which leads to a loss of angular momentum (Heger & Woosley 2003). The initial spin of neutron stars are possibly as low as 7-140 ms (Migliazzo et al. 2002; Kramer et al. 2003). The typical size of a neutron star is assumed to be around 20 km in diameter and with a mass somewhere between 1.1-2.5 $M_\odot$, although for simplicity it is often assumed to be around the Chandrasekhar limit of $1.4\,M_\odot$ (Lattimer & Prakash 2007; Lorimer & Kramer 2012; Tauris 2016).

1.2   Pulsars

The zoo of pulsars spans several wavelength regimes, from γ-ray to radio. Common to all pulsars is the geometry of the neutron star. It has a magnetic field, which is misaligned with respect to the rotation axis (see Fig. 1.1). The offset between the magnetic field poles and rotation axis is the reason why we observe pulsations, as long as the emission cone is in our line of sight. The pulses are generated by the modulation of the emitted radiation and not created by distortions of the neutron star itself.

1.2.1   Accreting X-ray Pulsars

If a neutron star is formed in a binary system, with a non-degenerate companion star, it is possible that this system will become an X-ray pulsar binary (Frank et al. 2002). In some X-ray binaries the companion is able to transfer material onto the neutron star. This happens through one of two scenarios, either Roche lobe overflow or wind accretion. Roche lobe overflow, which is often the mechanism in
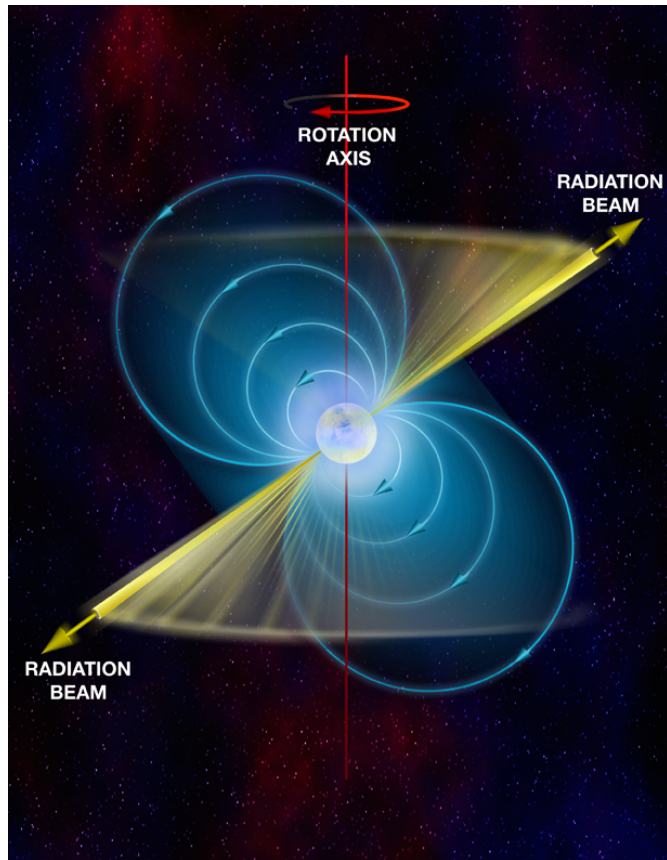
Figure 1.1: The basic geometry of a pulsar, where the magnetic field axis (north/south pole of the magnetic field) is misaligned with the rotational axis of the neutron star. Image credit: Bill Saxton, NRAO/AUI/NSF.

low mass X-ray binaries, can have three different causes: 1) the companion star expands on a nuclear evolution timescale, 2) the orbit shrinks, which is due to loss of angular momentum, by either magnetic breaking or gravitational radiation or 3) some other effects are present, e.g. mass ejection or spin-orbit coupling. Wind accretion happens when the donor star, during its stellar evolution, ejects some mass as a stellar wind, and parts of this material is captured by the neutron star and accreted onto the surface (Frank et al. 2002). Wind accretion is the accretion mechanism for pulsars in high mass X-ray binaries, and often also in symbiotic X-ray binaries. Due to the strong magnetic field of neutron stars, of $\sim 10^{7-15}$G, the accreted material will be channeled onto the magnetic poles of the neutron star, and material will fall on to the poles and not evenly spread out over the neutron star surface, creating hot spots. Due to the material falling onto the neutron star surface, energy is released, corresponding to ~ 200 MeV/baryon (Frank et al. 2002). If, as shown on Fig. 1.1, the magnetic axis and the rotation axis are misaligned, then it should be possible to detect the heated polar caps as X-ray pulses at a certain spin frequency. The accretion mechanism is though to be the driving force that spins up pulsars to milliseconds and reduce the magnetic field. It is not well known how the magnetic field decreases, but ideas range from simple decays to a burial of the magnetic field due to the accreted material (Taam & van den Heuvel 1986; Romani 1990; Cumming et al. 2001). Broadly speaking there are three types of X-ray pulsars; low mass X-ray binaries (LMXBs), high mass X-ray binaries (HMXBs) and intermediate mass X-ray binaries (IMXBs).

Low Mass X-ray Binaries

The first confirmed low mass X-ray binaries was discovered about ~ 50 years ago by Webster & Murdin (1972). Since then around 200 LMXBs have been discovered, however, pulsations are only observed in relatively few systems, which counts about 21 accreting millisecond X-ray pulsars (AMXPs), about 10 nuclear powered pulsars (powered by nuclear burning rather than accretion) and about 4 of the slower pulsars (e.g. 2A 1822−371, 4U 1626−67, GRO 1744−28 and Her X−1) (Wijnands & van der Klis 1998; Chakrabarty & Morgan 1998; Patruno & Watts 2012). The LMXB pulsar population is found to be in binaries with orbital periods between a few days, for the widest systems, to a few minutes, for the ultra compact systems (Patruno & Watts 2012). The companion mass in the LMXBs is $\leq 1.0\,M_\odot$ (Xu & Li 2007). The accretion process in LMXBs occurs via Roche lobe overflow and the creation of an accretion disc. The donor star in LMXB systems varies from main sequence stars, white dwarfs (WDs) and brown dwarfs (BDs). The typical magnetic field for LMXB pulsars is around 10^{11-13} G for the slow spinning pulsars and 10^{8-9} G for the AMXPs.

The accretion disc mechanism

When accretion onto a neutron star happens via Roche lobe overflow (see Fig. 1.2), the binary orbit is close to circular and the orbital period is described by

Figure 1.2: Roche Love overflow happens when the companion star expands beyond the Roche lobe, within which the material is gravitationally bound to the star. The overflow can then create an accretion disc around the neutron star. Image credit: Cosmos - Swinburne University.

keplerian motion:

$$P = 2\pi\sqrt{\frac{a^3}{GM_{tot}}} \tag{1.1}$$

where M_{tot} is the total mass of the two stars in the binary, a is the semi-major axis and G is the gravitational constant.

The Roche lobe overflow happens when the companion star fills out its Roche lobe and expands beyond the Roche lobe border, see Fig. 1.2. When the overflow happens, material is no longer gravitationally bound to the companion star, and it is free to pass through the first Lagrangian point and accrete onto the neutron star (Frank et al. 2002).

The material that is accreted carries a specific angular momentum, J. Due to the angular momentum, the material is not falling directly onto the neutron star, but settles in a disc around the neutron star. If gas pressure dominates the structure of the disc, then a geometrically thin and optically thick disc will be formed. This is known as an "α-disc" (Shakura & Sunyaev 1973; Ghosh & Lamb 1979). The optically thick and geometrically thin disc has a scale height, H, which is smaller than the radial extension of the disc. The viscosity (fluidity) of the α-disc is given by $\nu = c_s H$, where c_s is the speed of sound (Shakura & Sunyaev 1973). The disc rotates at a near Keplerian frequency,

$$\nu_K(r) = \frac{1}{2\pi}\sqrt{\frac{GM_{NS}}{R^3}} \tag{1.2}$$

M_{NS} is the mass of the neutron star and R is the radius of the gas element rotating in the disc. The accretion disc experiences turbulent viscosity and in that way the accretion disc losses energy through thermal emission and angular momentum is transported outwards. This will allow for material from the disc to spiral in towards the neutron star. The accretion flow in the inner regions of the

accretion disc is disrupted by the dipole magnetic field of the neutron star, which is described by $B \sim \frac{\mu}{R_{NS}^3}$, where μ is the magnetic moment. Accretion transfers angular momentum from the disc to the neutron star, and spins it up. The spin-up of a pulsar scales with the amount of mass that is accreted onto the star by $\dot{\nu} \propto \dot{M}_{acc}^{6/7}$, where $\dot{\nu}$ is the spin frequency derivative and $\dot{M}_{acc}$ is the rate at which the neutron star accretes material (Bildsten et al. 1997). For systems that become millisecond pulsars, the spin-up process is often referred to as the recycling scenario (Alpar et al. 1982).

Symbiotic X-ray Binaries

Symbiotic X-ray binaries (SyXBs) are a subclass of LMXBs, where the companion star is a post-main sequence low mass star (Kuranov & Postnov 2015). Most symbiotic X-ray binaries have a white dwarf (WD) primary star (Lü et al. 2012), however, a few systems do have a neutron star primary, e.g. GX 1+4 (See Chapter 3 of this thesis). The systems with a WD primary are only modest X-ray emitters (Corbet et al. 2008). SyXBs show flaring activity, which is typical for systems accreting from a stellar wind. This seems to be the case for e.g GX 1+4 (González-Galán et al. 2012; Kuranov & Postnov 2015).

High Mass X-ray Binaries

More than 100 high mass X-ray binaries are known in our Galaxy (Chaty 2011). HMXBs usually have a high mass OB type donor star, with a mass above $10\,M_\odot$ (Xu & Li 2007; Chaty 2011). Accretion in HMXBs typically happen through a slow and dense wind that the massive donor star expels. In rare occasions the HMXBs can form an accretion disc. A sub-class of HMXB are the so called Be X-ray binaries. They typically have a neutron star in a wide and eccentric orbit around a B0-B2e type star (this type of star show emission lines). The Be/X-ray binaries have a circumstellar disc or rather a de-cretion disc, where the neutron star passes through, and accretes material (Chaty 2011). In some Be/X-ray binaries the pulsar, is able to form and maintain an accretion disc, even after it leaves the de-cretion disc of the Be-star (See e.g. Chapter 4 of this thesis). The Be/X-ray binary pulsars typically exhibit type I and type II outbursts. The type I are periodic and come from the neutron star crossing the decreation disc. The type II outbursts are brighter and happen at any phase (Chaty 2011). There are about 50 known Be/X-ray binaries in our Galaxy.

Intermediate Mass X-ray Binaries

Intermediate mass X-ray binaries are systems with a donor star mass between the LMXBs and HMXBs, so about 1.0-$10\,M_\odot$ (Xu & Li 2007). There are only very few IMXBs observed, due to mass transfer via Roche lobe overflow being

rapid and unstable for IMXBs. The instability is mostly due to the large mass ratio of the stars in the binary, which will lead to a common envelope and in-spiral phase (Xu & Li 2007). The mass transfer in IMXBs is so unstable and fast, that it is expected to happen on a dynamical/thermal timescale. The accretion is thought to occur via an accretion disc, as the donor stars in this mass regime are not able to create strong winds that could account for the X-ray emission from the pulsar (van den Heuvel 1975; Xu & Li 2007). There is some evidence that suggests, that some of the companion stars of LMXBs could originate from an IMXB donor star. This is due to high intrinsic luminosity of the current low mass donor star, and that it is simply easier for a higher mass donor star to keep the neutron star in a binary system after the supernova explosion (Podsiadlowski et al. 2002).

1.2.2   Radio Pulsars

Radio pulsars cover a variety of different sources from isolated slow pulsars to millisecond pulsars in binary systems. A typical way to classify radio pulsars is with the $P - \dot{P}$ diagram, which shows the spin period (P) vs. the spin period derivative ($\dot{P}$) of radio pulsars. In the top right corner of Fig. 1.3 the young pulsars are found. These are often isolated systems, and the spin of the young pulsars is thought to be close to their birth spin (Lorimer & Kramer 2012). The young pulsars often have a high spin down rate due to the loss of their rotational kinetic energy via electromagnetic wave radiation and relativistic particle outflow. They are thought to spin down and end up in the graveyard zone, where it is predicted by theoretical models that radio pulsars will not exist. If the pulsar is in a binary system, with a companion star that will evolve to fill its Roche lobe, then the pulsar could spin up to become a millisecond pulsar (MSP), as the ones seen in the lower left corner on Fig. 1.3. These do not only have a faster spin, they also have a lower magnetic field and are old systems (Smarr & Blandford 1976; Srinivasan & van den Heuvel 1982; Manchester 2017).

The radio MSPs are believed to have formed through a recycling scenario, where pulsars are spun up through accretion (and thus angular momentum transfer) onto the neutron star in a LMXB (Alpar et al. 1982; Bhattacharya & van den Heuvel 1991).

The age and magnetic field of the $P - \dot{P}$ diagram is inferred from $\tau \propto P/\dot{P}$ and $B \propto \sqrt{P\dot{P}}$. In Fig. 1.3 the spin down luminosity is also indicated, and this is usually given by $\dot{E} \propto \dot{P}/P^3$, which is the rate at which the rotational energy is lost (Lorimer & Kramer 2012). The initial spin periods of pulsars are related to the spin period of the progenitors core, which is not well known (Faucher-Giguère & Kaspi 2006).

1.2.3   Spiders & Recycled Pulsars

Part of the binary millisecond pulsar population are found to be in close binaries, with an orbital period (P_b) $\lesssim 24\,$hr, and have relatively small companion stars (Chen et al. 2013). These systems are thought to ablate their companion star by
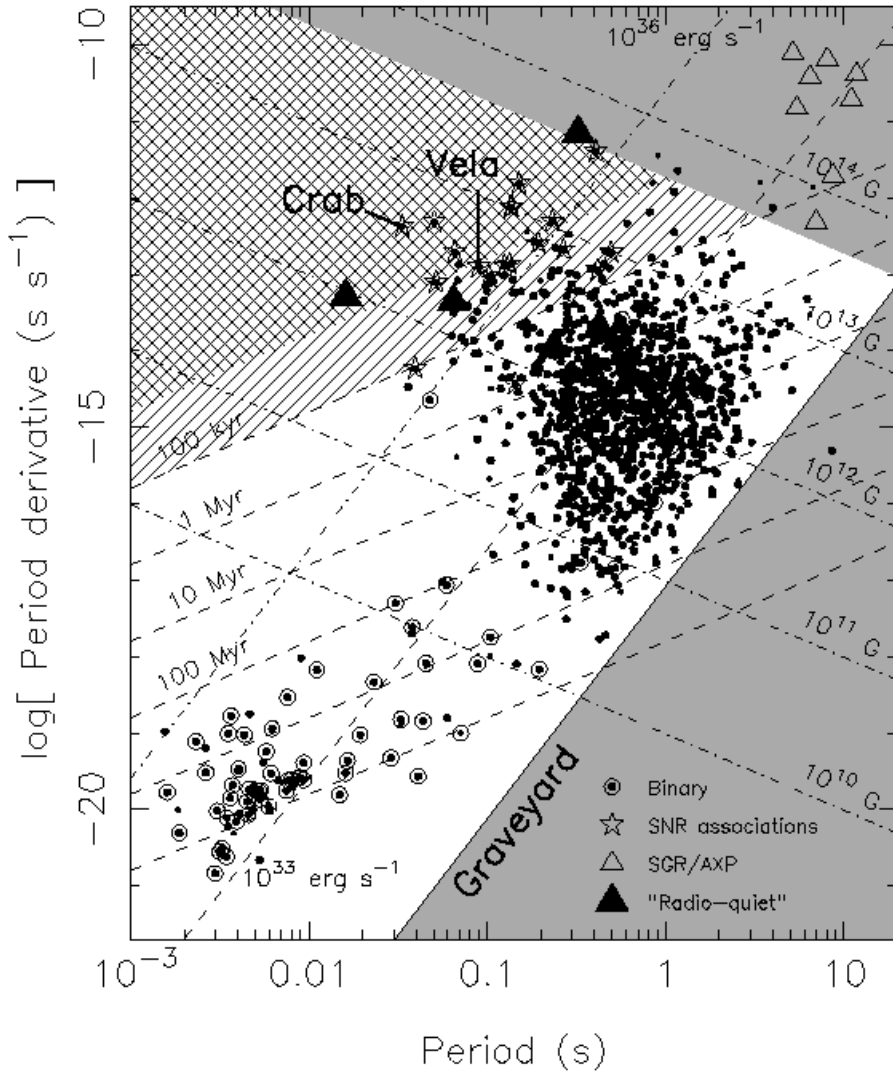
Figure 1.3: The P-$\dot{P}$ diagram of known radio pulsars. The upper area is occupied by the slow young radio pulsars and in the bottom left the old, recycled pulsars are shown. The dark grey areas are the graveyard zone for radio pulsars, within which very few radio pulsars are found. Image credit: Lorimer, D. & Kramer, M. - Handbook of Pulsar Astronomy, 2012

the pulsar electromagnetic radiation or the relativistic wind of the pulsar (Kiel & Taam 2013). The two types of spider systems, so called due to the ablation of the companion, are redback pulsars (RBPs) and black widow pulsars (BWPs). Some of the RBPs and BWPs show radio eclipses due to the outer layers of the companion star and the ablated material surrounding the companion star (Fruchter et al. 1988).

The general idea of the recycling mechanism is that pulsars in binary systems will, through accretion onto the neutron star, spin up the pulsar to millisecond spins. The spin-up happens through transfer of angular momentum in the accreted material. Furthermore, another part of the recycling scenario is that the magnetic field of the pulsar decreases (Alpar et al. 1982).

The spin period of recycled pulsars span 1.4-200 ms (Tauris 2016; Swiggum et al. 2015). The pulsar's spin is correlated with the mass of the companion star. The more massive and evolved the companion is when mass transfer begins, the slower the spin rate of the recycled pulsar will be. This is due to the mass transfer being much shorter for massive and evolved stars than for low mass stars (Tauris 2016).

Black Widow Pulsars

Black widow pulsars typically have small companion stars of less than $M_2 < 0.1\,M_\odot$ and a small magnetic field of $\sim 10^{8-9}$ G. The companion star is a semi-degenerate star, assumed to be similar to a brown dwarf (Chen et al. 2013). The first BWP was observed by Fruchter et al. (1988), since then about 40^1 systems have been found. The first two BWPs discovered, e.g. PSRs B1957+20 and J2051−0827, are unstable. The instability means that it is only possible to create a coherent, stable timing solution for short periods of time, months to years (Shaifullah et al. 2016; Lazaridis et al. 2011). There does, however, seem to be some BWPs that are stable, e.g. PSR J0023+0923, J2234+0944 and 2214+3000 (Arzoumanian et al. (2018) and Chapter 5 in this thesis).

Dependent on the size and configuration of the orbital period, the pulsar wind can interact with the ablated material form the companion star, and this produces an intra-binary shock, whose orientation can change with respect to the orbital phase. This is what creates the obscuration of the pulsed radio emission during the radio eclipses for some of the BWPs and RBPs (Roberts 2011).

Redback Pulsars

The first redback pulsar was found by D'Amico et al. (2001), and since then around 20 RBPs have been found. The RBPs have slightly larger companion masses than

---

[1]see e.g. `https://apatruno.wordpress.com/about/millisecond-pulsar-catalogue/` for both BWPs and RBPs.

the BWPs, of about 0.1-0.4 $M_\odot$ and the same low magnetic fields of about 10^{8-9} G (Chen et al. 2013). RBPs also differ from the BWPs with their less evolved companions. The companions are non-degenerate, suggesting that the RBPs are in the late stages of recycling (Roberts 2011). In 2009 a pulsar was discovered that linked the recycled pulsars to the LMXBs. It was PSR J1023+0038, which turned out to be a transitional system (Archibald et al. 2009; Roberts 2013). Transitional systems are binarys systems with a pulsar, that switch from being a LMXB to a radio pulsar in a cyclic way (Archibald et al. 2009; Papitto et al. 2013; Bassa et al. 2014; Roy et al. 2015). Observations from 2001 showed emission lines that indicated the presence of an accretion disc. In 2004 the emission lines were gone and radio pulsations were discovered (Roberts 2013).

1.3   Techniques

Timing of pulsars is a technique that tracks the time of arrivals (TOAs) of pulsars, recorded with an observatory, e.g. an X-ray or radio observatory, and then compares the TOAs with a predicted best-fit model (Lorimer & Kramer 2012; Desvignes et al. 2016). To track pulsations it is necessary to take into account the spin frequency of the pulsar (which is expressed as a Taylor series; $\nu(t) = \nu_0 + \dot{\nu}_0(t - t_0) + \frac{1}{2}\ddot{\nu}(t - t_0)^2...$ and to account for frequency dependent delays due to the ionized interstellar medium (IISM) (Lorimer & Kramer 2012).

1.3.1   Timing analysis

Timing analysis of pulsars is the essential tool in examining the basic properties (spin, orbital period, etc) of pulsars, and it is a tool that can help discover new properties of pulsars, and perhaps even gravitational wave signals (Lorimer & Kramer 2012; Janssen et al. 2015). When using timing analysis, several influences on the pulse time of arrival are taken into account, and propagation delays affecting the pulsar signal should be accounted for. First of all, the pulse time of arrivals need to be corrected to an inertial reference frame, to take the Earth movement around the Sun into account. The pulsar observations, both in X-ray and radio, are barycentered, meaning the pulsar position and movement is referred to the solar system barycenter. Furthermore, the planets in the solar system also have an effect on the signal we observe, and we need to correct the data for their relative positions to the solar system barycentre. Ephemerides for the planet positions are provided by the Jet Propulsion Laboratory (JPL). When the corrections are applied to the pulsar data, the data is folded to increase the signal to noise of the pulsations. So far, the above is valid for both X-ray and radio pulsars. However, to create TOAs for a radio pulsar it is necessary to cross-correlate the data with a template pulse profile. For X-ray pulsars a sinus curve, or harmonic decomposition of the signal, is used instead of a fixed template (Hartman et al. 2008). A harmonic decomposition will avoid that the phase and amplitude variability, observed in these pulsars, create artificial variations when creating the TOAs. Using a fixed profile for X-ray pulsars could thus introduce artificial variability in the TOAs.
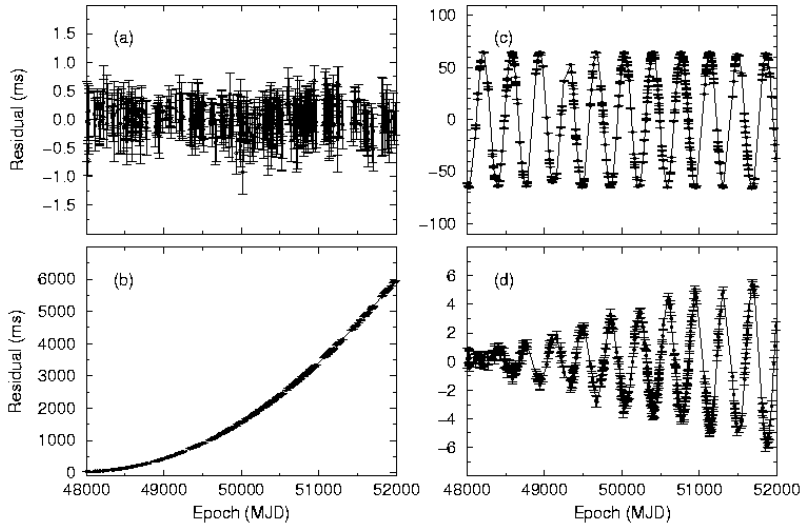
Figure 1.4: Residuals showing missing parameters from a timing solution, here PSR B1133+16 is used as an example. Panel *a* shows a perfect timing solution, with residuals having a Gaussian distribution around zero. Panel *b* shows a missing or underestimated $\dot{P}$. Panel *c* shows an off set in position, and panel *d* shows the effect of not taking the pulsars proper motion into account. Image Credit: Lorimer & Kramer (2012).

Radio pulsars have very stable pulse profiles, and it is thus a fixed template that is correlated to the data when creating the TOAs. The rotational phase of any pulsar is described by:

$$\phi(t) = \phi_0 + \nu_0(t - t_0) + \frac{1}{2}\dot{\nu}(t - t_0)^2 + \frac{1}{6}\ddot{\nu}(t - t_0)^3... \qquad (1.3)$$

ϕ_0 it the pulse phase at time t_0, and the phase is measured in cycles. For any timing solution, the desired purpose is to be able to gain insight into the astrometric parameters (position, proper motion, parallax etc.), spin parameters (spin frequency and the derivatives of the spin frequency) and binary parameters (orbital period, eccentricity, semi-major axis etc.) (Lorimer & Kramer 2012). The aim is to find a phase-coherent timing solution, which accounts for all rotations of the pulsar between different observations. When using long observations, it is common that derivatives of parameters need to be included in the timing solutions. Incorrect timing solutions introduce systematic structures in the post-fit residuals, from which it is possible to detect which parameter is missing or needs to be adjusted, see Fig. 1.4.
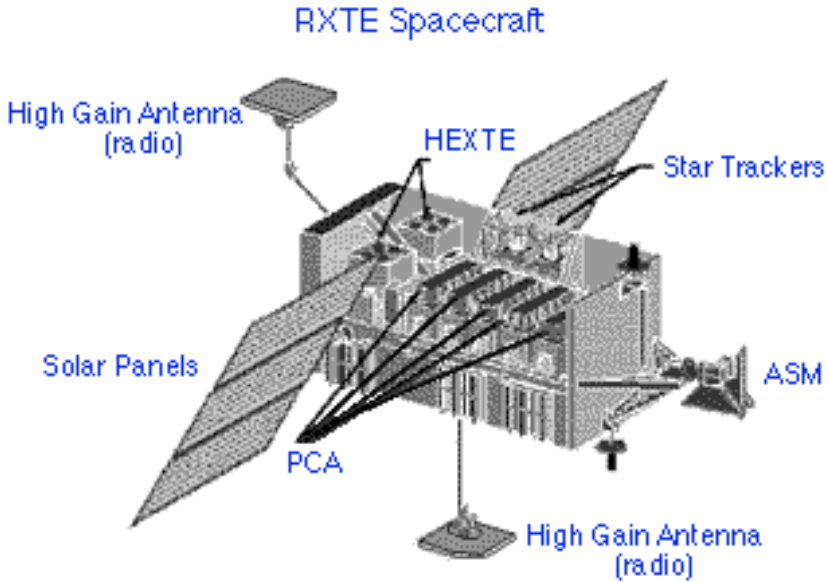
Figure 1.5: The Rossi X-ray Timing Explorer (*RXTE*) was an X-ray telescope which was active from 1995 to 2012.Image Credit: NASA.

1.4   Observatories

In this thesis data from several observatories has been used, and below is a short description of the different telescopes.

1.4.1   RXTE

The *Rossi X-ray Timing Explorer* (*RXTE*), see Fig. 1.5 , was a NASA controlled X-ray satellite, which was launched on 30. December 1995. The telescope could cover timescales of milliseconds to months and had a spectral range of 2-250 keV. *RXTE* was decommissioned in 2012. The telescope carried two pointed instruments. The proportional Counter Array (PCA), which had a collecting area of 6500 cm^2 and which covered the low energy range of the telescope, 2-60 keV. The other pointed instrument was the High Energy X-ray Timing Experiment (HEXTE) which had a collecting area of 2×800 cm^2 and covered the upper range of the energy bands, 15-250 keV. In addition to this, *RXTE* also carried the All-Sky Monitor (ASM), which could scan about 80% of the sky at every orbit.

Figure 1.6: *XMM-Newton* is an ESA space telescope. It was launched in 1999 and is still operating. Image Credit: ESA.

1.4.2 XMM-Newton

The *X-ray Multi-Mirror Mission* (*XMM-Newton*) is an ESA controlled mission, launched on 10. December 1999 (see Fig. 1.6). There are three X-ray instruments on board *XMM-Newton* (RGS, EPIC-pn and EPIC-MOS) and an optical monitor (OM). The RGS consists of two Reflection Grating Spectrometer readout cameras and EPIC-MOS consists of two imaging detectors (MOS1 and MOS2), which are both CCD cameras, and MOS stands for Metal Oxide Semi-conductor. The EPIC-pn has an unobstructed beam and it uses pn CCDs. The EPIC cameras are able to perform sensitive imaging over the 30 arcmin telescope field of view and in the energy range of 0.15-15 keV. The OM instrument covers 160-550 nm and has a resolution down to magnitude +24.5. The telescope has a collecting area of 1475 cm^2 at 1.5 keV and 580 cm^2 at 8 keV. The relatively large collecting area and the ability to take long and uninterrupted exposures, make it a highly sensitive X-ray telescope.

1.4.3 Pulsar Timing Arrays

There are three collaborations around the world that aspire to observe gravitational waves using pulsar timing. Via precise timing of pulsars it should be possible to

detect signatures in the pulsar timing residuals which belong to gravitational waves crossing the pulsars (Desvignes et al. 2016). By using an array of pulsars, meaning different pulsars in different places on the sky, it should be possible to detect the characteristic quadrupolar, and higher order, angular signatures that gravitational waves crossing the sky exhibits. The quadrupolar behaviour of the gravitational wave signal should be distinguishable from the lower order terms that pulsars otherwise exhibit (Foster & Backer 1990). Furthermore, using an array of pulsars is expected to increase the signal to noise ratio of the gravitational wave signal in the timing residuals and by cross-correlating the signal between the pulsars in the array, it is possible to distinguish between the GW signal and other signals that may be present in the timing of the individual pulsars (Lentati et al. 2015).

The efforts to time an array of pulsars precisely is undertaken by the European Pulsar Timing Array (EPTA), North American Nanohertz Observatory for Gravitational Waves (NANOGrav) and the Parkes Pulsar Timing Array (PPTA), all three are collectively know as the International Pulsar Timing Array (IPTA). The EPTA uses five telescopes spread across Europe; the Effelsberg Telescope in Germany, the Lovell telescope at Jodrell Bank in the UK, the Nançay Radio Telescope in France, Westerbork Synthesis Radio Telescope (WSRT) in the Netherlands and the Sardinia Radio Telescope in Italy.

1.4.4 European Pulsar Timing Array Telescopes

The 5 telescopes used by the EPTA are very different telescopes. WSRT consists of 14 individual dish antennas, each with a diameter of 25 m, see panel *a* on Fig. 1.7, and was completed in 1970, with later upgrades. Twelve of the dishes are at permanent positions and at the eastern side of the telescope are two movable antennas. For the observations used in this thesis the WSRT had a frequency setup available of 345-1400 MHz. The total frequency range of WSRT is 120-8300 MHz.

The Effelsberg telescope is a 100 m single dish telescope, see panel *b* on Fig. 1.7. The telescope was first used in 1972 and has since then continuously been upgraded. The Effelsberg observes at a frequency of 300-9000 MHz, however, in this thesis it has been used at a configuration observing at 1400-2500 MHz.

The Nançay Radio Telescope was inaugurated in 1965 and is a transit instrument of the Kraus-type design, meaning it has two mirrors, a flat tilting primary mirror that is ten panels of 20 m long and 40 m tall (See panel *c* on Fig. 1.7). Its secondary mirror is 460 m south of the primary, which has the shape of part of a circle, which would have a radius of 560 m. The observing frequency of the telescope is 1060-3500 MHz and in this thesis the frequency range used is 1400-1500 MHz.

The Lovell telescope is the largest radio telescope at Jodrell Bank, and it is a single dish telescope with a diameter of 76.2 m. The telescope has been actively working since 1957 (See panel *d* on Fig. 1.7). The observing frequency spans
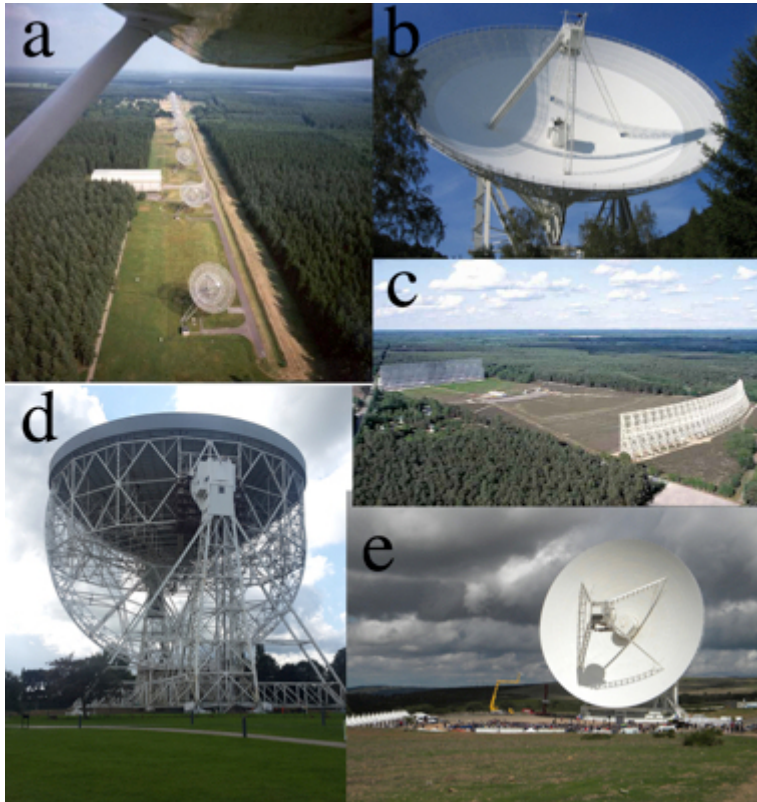
Figure 1.7: The European Pulsar timing array telescopes. a) The Westerbork Radio Synthesis Telescope, b) Effelsberg Radio Telescope, c) Nançay Radio Telescope, d) Lovell Telescope and e) The Sardinia Radio Telescope. Image credit: ASTRON (WSRT), EPTA (EFF), MPIfR BONN (Nançay), Private photo (Lovell), Sardinia Radio Telescope (SRT).

408-6000 MHz and the frequency setup used in this thesis was 1400-1500 MHz.

The last telescope of the EPTA is the Sardinia Radio Telescope (SRT), which was build in 2011 (See panel *e* on Fig. 1.7). It has a 64 m primary mirror and a 7.9 m secondary mirror. The frequency coverage is 300-1000 MHz.

1.5 This thesis

In this thesis I examine some of the peculiar behaviours that some pulsars show. I look at both accreting and radio pulsars in binary systems and try to give explanations to the behaviour of the different systems.

In Chapter 2 we look at the persistent low mass X-ray binary pulsar 2A 1822-371. It is an eclipsing system with an accretion disc corona and an orbital period of 5.57 hr. In this chapter we study the evolution of the pulsar and constrian the geometry of the system. We present a possible explanation for the orbital evolution of the system where we suggest that 2A 1822-371 is a source with a possible super-Eddington mass transfer rate. We used 13 years of *RXTE* data.

Chapter 3 is a study of whether there is pulse phase - flux correlation in the symbiotic X-ray pulsar GX1+4. A pulse phase - flux correlation has previously been found in accreting millisecond pulsars and in this chapter we thus tested if there is a smiliar correlation in binaries with high magnetic field and slow rotating pulsars. In this chapter we used *RXTE* data.

In Chapter 4 we examined the Be/X-ray transient 4U 0115+63 after the source had undergone a giant type-II outburst. The source did not immediately settle into its quiescent state, but instead it settled in a meta-stable plateau phase in which the luminosity then slowly decayed. *XMM-Newton* was used to observe the system during the meta-stable plateau phase and we found that there is an emitting region, suggesting a hot spot on the surface of the pulsar. The hot-spot was confirmed form the discovery of pulsations.

For Chapter 5 we examined three stable black widow pulsars, PSR J0023+0923, J2214+3000 and J2234+0944. The first BWPs observed have unstable timing solutions and show variability in the orbital parameters. In this chapter we present long-term timing solutions for the three stable BWPs, using four of the five EPTA telescopes. We discuss possibilities as to why these particular systems are stable and the first observed BWPs are unstable.

Bibliography

Alpar M. A., Cheng A. F., Ruderman M. A., Shaham J., 1982, Nature, 300, 728

Archibald A. M., et al., 2009, Science, 324, 1411

Arzoumanian Z., et al., 2018, preprint, (arXiv:1801.01837)

Baade W., Zwicky F., 1934, Physical Review, 46, 76

Bassa C. G., et al., 2014, MNRAS, 441, 1825

Bhattacharya D., van den Heuvel E. P. J., 1991, Phys. Rep., 203, 1

Bildsten L., et al., 1997, ApJ, 113, 367

Chakrabarty D., Morgan E. H., 1998, Nature, 394, 346

Chaty S., 2011, in Schmidtobreick L., Schreiber M. R., Tappert C., eds, Astronomical Society of the Pacific Conference Series Vol. 447, Evolution of Compact Binaries. p. 29 (arXiv:1107.0231)

Chen H.-L., Chen X., Tauris T. M., Han Z., 2013, ApJ, 775, 27

Corbet R. H. D., Sokoloski J. L., Mukai K., Markwardt C. B., Tueller J., 2008, ApJ, 675, 1424

Cumming A., Zweibel E., Bildsten L., 2001, ApJ, 557, 958

D'Amico N., Possenti A., Manchester R. N., Sarkissian J., Lyne A. G., Camilo F., 2001, ApJ, 561, L89

Desvignes G., et al., 2016, MNRAS, 458, 3341

Faucher-Giguère C.-A., Kaspi V. M., 2006, ApJ, 643, 332

Foster R. S., Backer D. C., 1990, ApJ, 361, 300

Frank J., King A., Raine D. J., 2002, Accretion Power in Astrophysics: Third Edition

Fruchter A. S., Stinebring D. R., Taylor J. H., 1988, Nature, 333, 237

Ghosh P., Lamb F. K., 1979, ApJ, 234, 296

González-Galán A., Kuulkers E., Kretschmar P., Larsson S., Postnov K., Kochetkova A., Finger M. H., 2012, A&A, 537, A66

Hartman J. M., et al., 2008, ApJ, 675, 1468

Heger A., Woosley S. E., 2003, in Ricker G. R., Vanderspek R. K., eds, American Institute of Physics Conference Series Vol. 662, Gamma-Ray Burst and Afterglow Astronomy 2001: A Workshop Celebrating the First Year of the HETE Mission. pp 214–216 (arXiv:astro-ph/0206005)

Heger A., Woosley S. E., Langer N., Spruit H. C., 2004, in Maeder A., Eenens P., eds, IAU Symposium Vol. 215, Stellar Rotation. p. 591 (arXiv:astro-ph/0301374)

Hewish A., Bell S. J., Pilkington J. D. H., Scott P. F., Collins R. A., 1968, Nature, 217, 709

Hulse R. A., Taylor J. H., 1975, ApJ, 195, L51

Janssen G., et al., 2015, Advancing Astrophysics with the Square Kilometre Array (AASKA14), p. 37

Kiel P. D., Taam R. E., 2013, Ap&SS, 348, 441

Kramer M., Lyne A. G., Hobbs G., Löhmer O., Carr P., Jordan C., Wolszczan A.,

2003, ApJ, 593, L31

Kuranov A. G., Postnov K. A., 2015, Astronomy Letters, 41, 114

Lattimer J. M., Prakash M., 2007, Phys. Rep., 442, 109

Lazaridis K., et al., 2011, MNRAS, 414, 3134

Lentati L., et al., 2015, MNRAS, 453, 2576

Lorimer D. R., Kramer M., 2012, Handbook of Pulsar Astronomy

Lü G.-L., Zhu C.-H., Postnov K. A., Yungelson L. R., Kuranov A. G., Wang N., 2012, MNRAS, 424, 2265

Manchester R. N., 2017, Journal of Astrophysics and Astronomy, 38, 42

Migliazzo J. M., Gaensler B. M., Backer D. C., Stappers B. W., van der Swaluw E., Strom R. G., 2002, ApJ, 567, L141

Papitto A., et al., 2013, Nature, 501, 517

Patruno A., Watts A. L., 2012, preprint, (arXiv:1206.2727)

Podsiadlowski P., Rappaport S., Pfahl E. D., 2002, ApJ, 565, 1107

Roberts M. S. E., 2011, in Burgay M., D'Amico N., Esposito P., Pellizzoni A., Possenti A., eds, American Institute of Physics Conference Series Vol. 1357, American Institute of Physics Conference Series. pp 127–130 (arXiv:1103.0819)

Roberts M. S. E., 2013, in van Leeuwen J., ed., IAU Symposium Vol. 291, Neutron Stars and Pulsars: Challenges and Opportunities after 80 years. pp 127–132 (arXiv:1210.6903)

Romani R. W., 1990, Nature, 347, 741

Rosswog S., Brüggen M., 2011, Introduction to High-Energy Astrophysics

Roy J., et al., 2015, ApJ, 800, L12

Shaifullah G., et al., 2016, MNRAS, 462, 1029

Shakura N. I., Sunyaev R. A., 1973, A&A, 24, 337

Shearer A., Golden A., 2002, in Becker W., Lesch H., Trümper J., eds, Neutron Stars, Pulsars, and Supernova Remnants. p. 44 (arXiv:astro-ph/0208579)

Smarr L. L., Blandford R., 1976, ApJ, 207, 574

Smith D. A., Guillemot L., Kerr M., Ng C., Barr E., 2017, preprint, (arXiv:1706.03592)

Srinivasan G., van den Heuvel E. P. J., 1982, A&A, 108, 143

Swiggum J. K., et al., 2015, ApJ, 805, 156

Taam R. E., van den Heuvel E. P. J., 1986, ApJ, 305, 235

Tauris T. M., 2016, Mem. Soc. Astron. Italiana, 87, 517

Webster B. L., Murdin P., 1972, Nature, 235, 37

Wijnands R., van der Klis M., 1998, Nature, 394, 344

Xu X.-J., Li X.-D., 2007, A&A, 476, 1283

van den Heuvel E. P. J., 1975, ApJ, 198, L109